GEOMATICS AND ENVIRONMENTAL ENGINEERING • Volume 19 • Number 5 • 2025

https://doi.org/10.7494/geom.2025.19.5.5

Krzysztof Będkowski[1]

# Manual versus Digital Classification of UAV Images in Oak Phenological Studies

**Abstract:** This research concerns the phenological phenomenon of the autumn discolorations of sessile oak leaves as the trees prepare for winter dormancy. Sessile oak trees were categorized into five classes according to the general colors of their crowns: from green to brown. Low-altitude UAV-acquired images from the visible B, G, and R bands were used, compared, and evaluated against the results of several classification methods: those that were carried out in the field, visually based on orthomosaic observations, and four variants of digital classification.

The analysis showed that those methods that were based on observer assessments were highly subjective. At the same time, there was also the problem of the reference data to which the results of the individual methods could be referred. It was expected that the analyzed phenomenon of tree-crown discoloration would be better visible in aerial photographs than in field observations; However, visual color classifications using orthomosaics can be too subjective (as has been shown). It is recommended to use supervised digital classification with a careful selection of reference (training) objects.

To switch from pixel-classification results to individual tree classifications, a novel approach was adopted in which the class value that was most abundant within the images of each canopy (determined by the supervised classification method selected) could be used. Among the supervised digital-classification methods that were applied, the results that were closest to the classification performed in the field were obtained by using the ML and Fisher algorithms (followed by kNN).

**Keywords:** oak, phenology, UAV, image classification

Received: August 11, 2024; accepted: June 19, 2025



[1] University of Lodz, Faculty of Geographical Sciences, Łódź, Poland, email: krzysztof.bedkowski@geo.uni.lodz.pl, https://orcid.org/0000-0001-7945-343X

## 1. Introduction

Each year, the cyclical phenomena in the natural environment that result from the variability of the seasons can be observed: plants develop and go through successive phases of development in a specific order, with some undergoing the process later (benefitting from the delays in the developments of other plants). Within several species of trees, differences in the developments of individual trees can also be observed; however, the causes of these phenomena are not fully understood [1–6]. The potential impact of habitat microdiversity – fertility and access to water, reactions to the presence of pathogens (mainly insects) – is indicated [7–13]. Research on the course of phenological phenomena has become very important due to the clear impact that global climate change has on individual tree species [14–16].

Among the economically important species of deciduous trees, such differences in the phenological developments of spring and autumn specimens are clearly visible in the beech *Fagus sylvatica* L., oaks (of which, there are three native species in Poland; namely, the pedunculate oak [*Quercus robur* L.], sessile oak [*Quercus petraea* (Matt.) Liebl.], and downy oak [*Quercus pubescens* Willd.] (which occurs at only one very small locality), and European ash trees (*Fraxinus excelsior* L.).

The phenomena that occur in the spring are more often the subjects of scientific phenological studies; for this reason, they are better understood than those that occur in the autumn. Studies on the course of phenological phenomena may cover vast areas; for this purpose, aerial-remote-sensing and satellite-remote-sensing methods are very often used [17, 18, 20–23, 26, 27]. In the case of small areas or small groups of trees, images that are obtained using unmanned aerial vehicles are useful [20–22].

The phenological phenomena that occur in the autumn are related to the preparations of trees for winter dormancy; this is expressed externally in changes in their leaves' colors and, later, in the amounts of assimilation apparatus. Without going into the details of the biochemical transformations that take place in the leaves [23–31], it can certainly be noticed that the leaves change their colors from green through various shades of yellow (sometimes, also red) to brown. In some species (e.g., the larch [*Larix* sp.]), the needles fall off after reaching a yellow color, while red can often be seen in maples (*Acer* sp.). According to many years of observations, two species of oaks undergo color transformations in the following cycle: green (G), yellow (Y), and brown (B); the red color (which can be attributed to an entire tree) is basically not observed in the oaks. In addition to the indicated colors, it is also possible to distinguish intermediate colors; e.g., green/yellow (G/Y) and yellow/brown (Y/B).

From the remote-sensing level, the diversity of the colors of the assimilation apparatus of trees is easily observable. Images that are recorded in the visible bands (B, G, R) or within the infrared (IR) range may be used for crown-color analysis. Image processing may be carried out using many different techniques; among these, spectral indices and digital classification (in its various variants – supervised, unsupervised, multispectral, or object-oriented) seem to be the most useful.

This paper compares the classifications of images that were obtained with the use of a camera that was carried by a UAV for the purpose of studying the course of the phenomenon of the autumn discoloration of the assimilation apparatus in sessile oak. The consistency of the results of four variants of numerical classification was checked, along with the results of visual classifications and classifications that were performed in the field. The advantages and disadvantages of numerical, manual, and visual solutions were discussed. Finally, a numerical way of switching from pixel classification to the classifications of whole tree crowns was also proposed.

## 2. Materials and Methods

### 2.1. Study Area

The research concerned a sessile oak stand (*Quercus petraea* [Matt.] Liebl.) that was located in central Poland (51.763267 N, 20.115792 E); this featured trees that were about 85 years old that had an average breast-height-diameter (BHD) of 27 cm and an average height of 24 m. In the main stand, there was a small number of Scots pines (*Pinus sylvestris* L.) with no second story nor undergrowth; in the understory layer, there were occasionally common hazels (*Corylus avellana* L.). The undergrowth layer was relatively poor in terms of the species composition; in some places, the vegetation cover was discontinuous.

### 2.2. Low-Altitude UAV Images

Aerial images were recorded on October 27 using an AVI-1 drone – an electrically powered airframe that carried two Sigma DP2 cameras; one of the cameras recorded images in the visible range (RGB), while the other was modified to record the infrared (IR) channel [32]. In this study, only RGB images were used; these were transformed with EnsoMOSAIC software into an orthomosaic with a spatial resolution (understood as the ground-sampling distance – GSD) of 0.15 m.

### 2.3. Field Phenological Observations

In the studied stand, permanent experimental plots were located; these consisted of the appropriate markings and precise geodetic measurements of the locations of all of the trees that formed the main stand as well as their basic dendrological characteristics: BHD, heights, and crown diameters. At the same time, one observer classified each of the 417 oak trees into one of five classes based on their dominant leaf colors: green (G), green/yellow (G/Y), yellow (Y), yellow/brown (Y/B), and brown (B). The distinguished color classes indicated the degrees of the advancements of the process of the trees' transitions to winter dormancy [20–22].

## 2.4. Aerial Photo Processing

In the RGB orthomosaic, the crown contours of all of the trees that were located on the trial plots were identified and manually digitized (Fig. 1a). The next step was to classify the oak crowns into the five color classes as before. The classifications were performed visually based on subjective assessments that were performed by the observer and then repeated in four variants of digital supervised classification. In the digital variant, a total of 25 carefully selected trees (i.e., five for each color class) were adopted as models (Fig. 1b).

a) b)

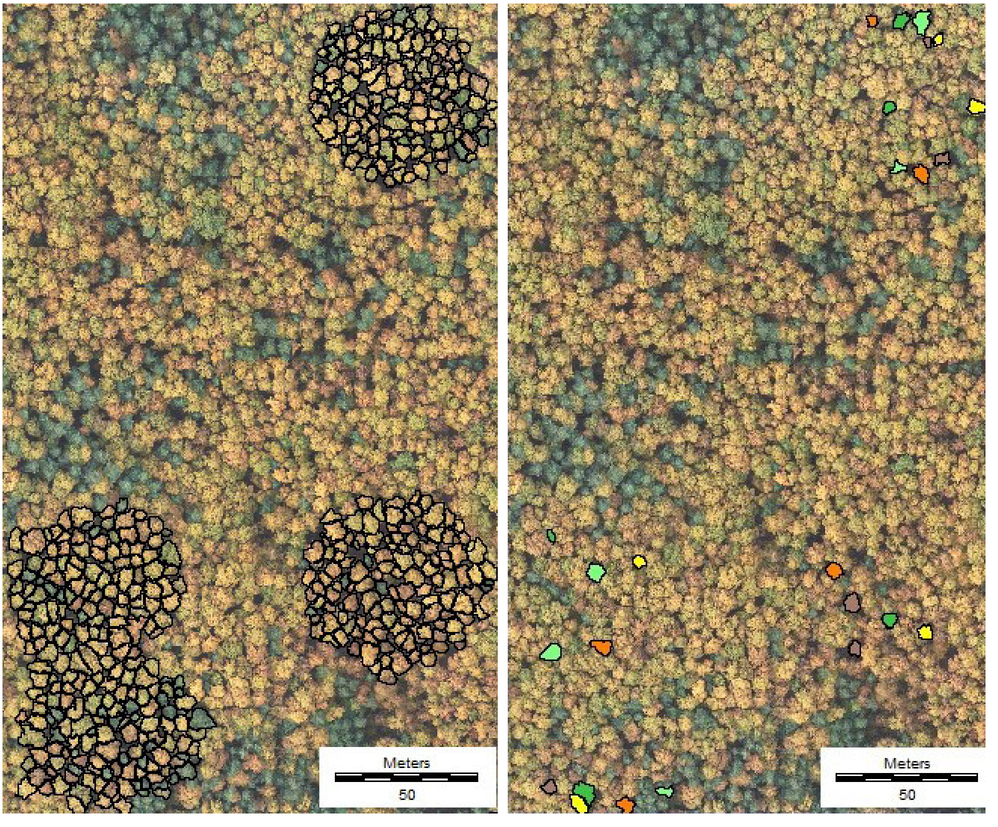


**Fig. 1.** Sample plots with marked tree crown ranges (a);
tree crowns selected as references in supervised classification (b)

Digital classification was performed using the minimum distance (MD), maximum likelihood (ML), Fisher, and k-nearest neighbors (kNN) algorithms. TerrSet® software was also used [33]. The illustrative materials that are included in the following sections of this article are limited to one research area in order to avoid unnecessary increases in the length of the paper. The numerical data that is contained in the attached tables accurately present the obtained results.

# 3. Results

## 3.1. Results of Field Phenological Observations

An observer in the field classified the trees by assigning each tree into one category of leaf color (Fig. 2a, Table 1).

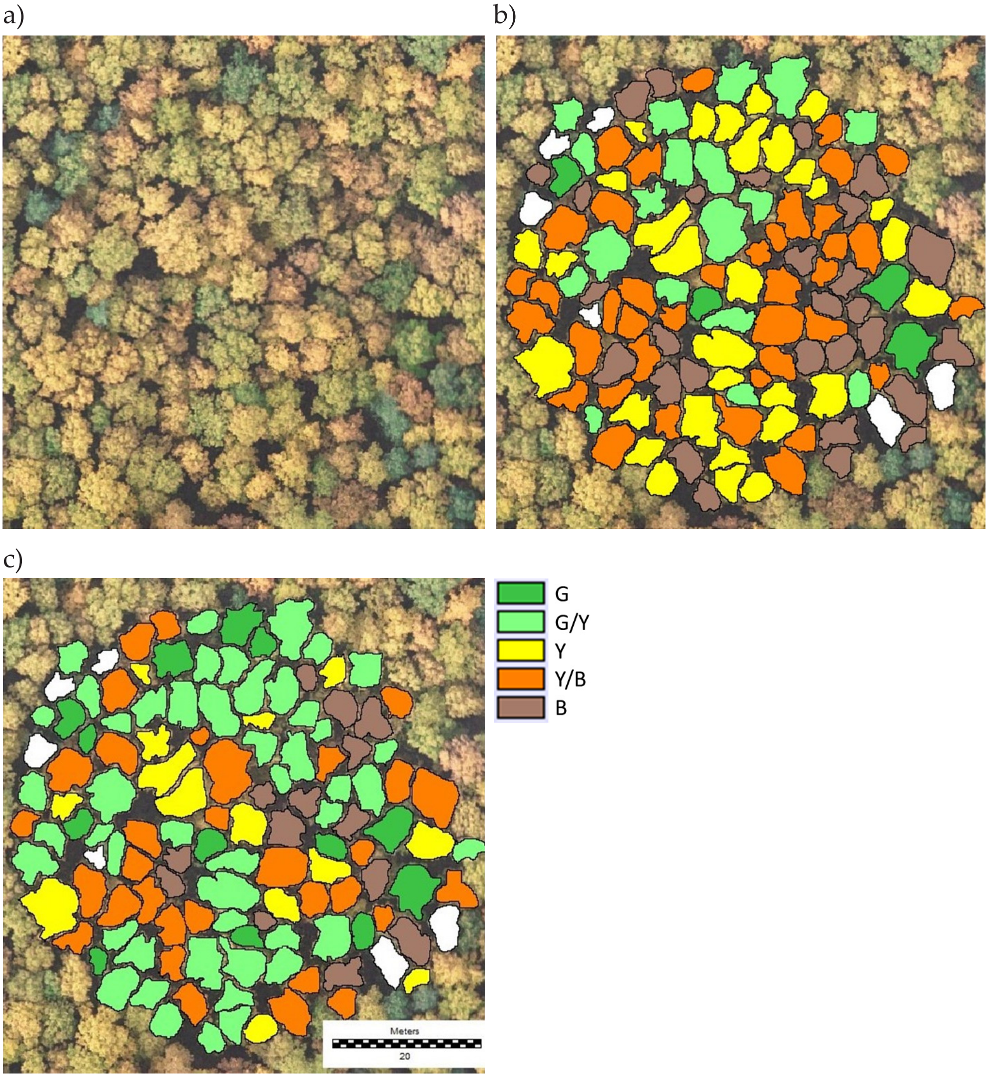


**Fig. 2.** One research area: oak crowns visible in orthomosaic that was made in October 2011 (a); results of classification performed in field (b); results of visual classification performed on orthomosaic (c); dominant color of crowns marked by attached color scale; unclassified trees (marked as white polygons) were Scots pines (orthomosaic section covered area of approx. 60 m × 60 m)

The vast majority of the trees had assimilation apparatus that were colored uniformly; i.e., one color throughout the entire crown. In the events of differences in the colorings between the upper and lower parts of the tree crown, the color of the upper part determined the final pass, as this part of the tree crown was also visible in the aerial photographs; thus, good compliance of the terrain classification was ensured with the classifications that were taken in the aerial photographs. No other differences in color could be observed among the studied trees – if the colors changed, this was only in the vertical gradient.

### 3.2. Results of Manual (Visual) Classification Performed with Use of RGB Orthomosaic

During the classifications that were performed visually on the aerial photographs (Fig. 2c, Table 1), the observer first marked the crowns of the trees; these were classified as green (G) and brown (B), then yellow (Y), and finally as the intermediate colors (G/Y and Y/B). Although the field and photo observations were made by other observers (compare the three parts of Figure 2), one can notice a certain agreement between the two classifications. Detailed data for the entire research material is included in Tables 2 and 3.

### 3.3. Results of Digital Supervised Classification of RGB Orthomosaic

In the supervised classification, the first assessment was carried out for the signatures of the oaks that were selected as the model for the five color classes. For this purpose, tools that are commonly used in remote sensing were used; i.e., a signature comparison chart (Fig. 3), scattergrams (Fig. 4), and separability measures (Table 1).

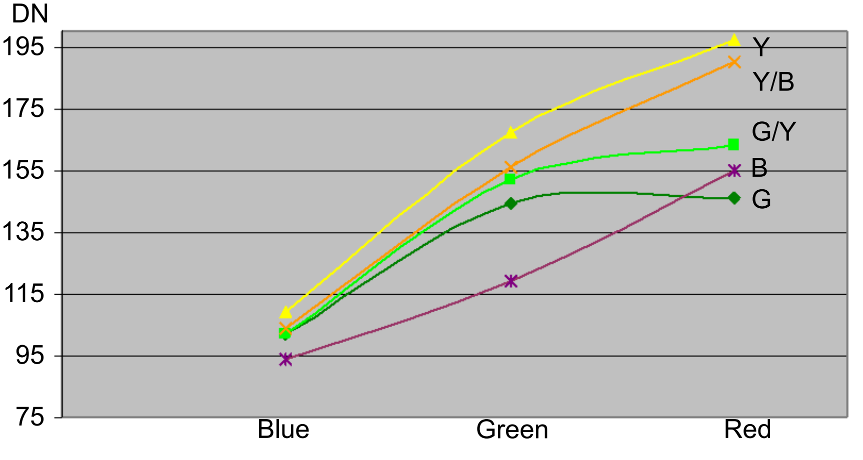


**Fig. 3.** Signature comparison chart for 25 oaks that were selected as training objects for five color classes of assimilation apparatus: on horizontal axis, orthomosaic spectral bands are marked (B, G, R); on vertical axis, average values of image brightness in crowns of model trees are placed

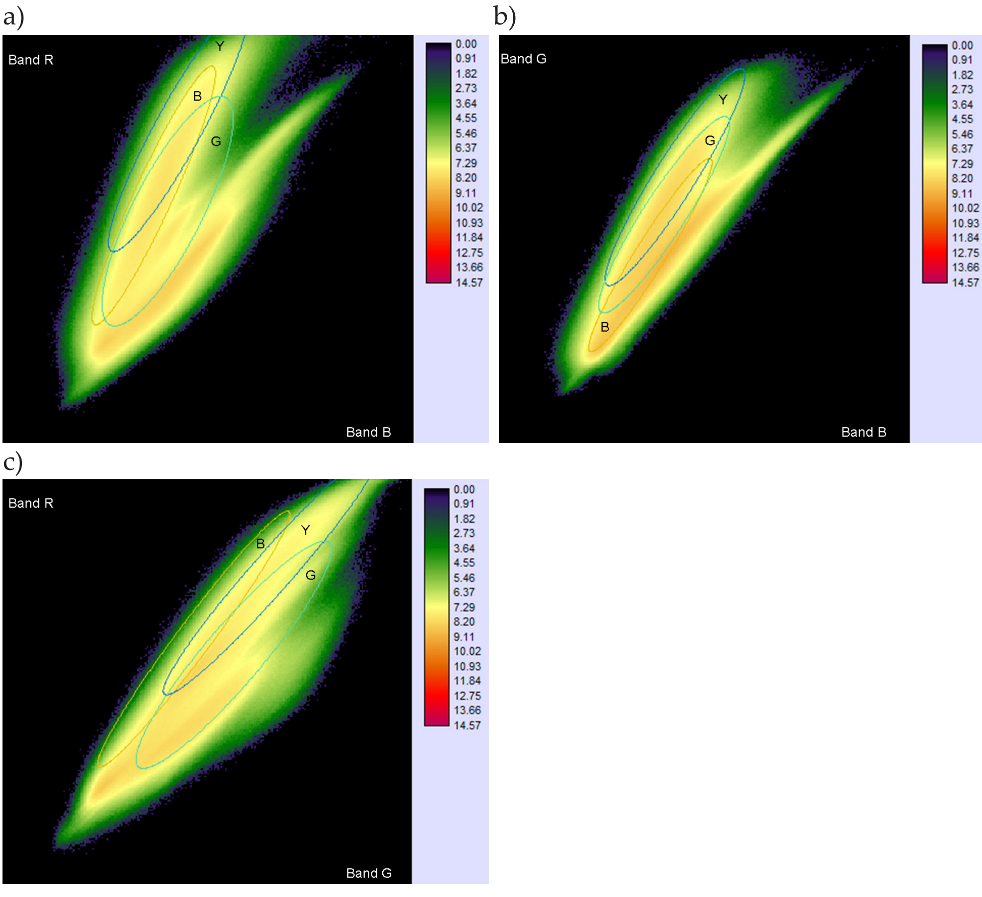


**Fig. 4.** Scattergrams showing spreads of pixel values of orthomosaic spectral bands: ellipses indicate spread ranges of pixel values for each color class of tree canopy selected as reference for digital classification; for better visibility, only ellipses for G, Y, and B oak classes are shown (logarithmic scale used in legend)

A comparison of the average brightness values of the images (Fig. 3) shows that the greatest differences among the oaks that belonged to the individual classes occurred in the red channel (R), followed by the green channel (G). The highest brightness values were recorded in those oaks that belonged to the group of trees with yellow crowns (Y), while the lowest values were in those oaks that belonged to the group with brown crowns. In general, the brightness of the images increased from the oaks with green crowns (G) to yellow/green (G/Y), then to yellow (Y); this decreased in the Y/B and B trees.

According to the scattergrams (Fig. 4), the ellipses of the scatter of the pixel values that belonged to the trees from the different classes of crown colors overlapped to some extent. In the figure, the ellipses for the G/Y and Y/B classes (which occupied intermediate positions) are not marked (for better visibility).

**Table 1.** Measures of signature separability

| Bhattacharyya Distance | | | | |
|---|---|---|---|---|
| Signature | G/Y | Y | Y/B | B |
| G | 136,961.47 | 1,205,049.32 | 821,316.75 | 249,689.30 |
| G/Y | – | 586,326.81 | 323,794.03 | 416,241.78 |
| Y | – | – | 72,555.12 | 1,598,317.51 |
| Y/B | – | – | – | 1,034,097.96 |
| Divergence | | | | |
| Signature | G/Y | Y | Y/B | B |
| G | 1.16 | 8.00 | 11.45 | 19.18 |
| G/Y | – | 3.55 | 6.27 | 17.32 |
| Y | – | – | 0.54 | 11.07 |
| Y/B | – | – | – | 6.65 |
| Transformed Divergence | | | | |
| Signature | G/Y | Y | Y/B | B |
| G | 270.76 | 1263.98 | 1521.82 | 1818.04 |
| G/Y | – | 716.40 | 1086.45 | 1770.40 |
| Y | – | – | 130.39 | 1499.01 |
| Y/B | – | – | – | 1129.42 |

The overlapping of the ellipses (Fig. 4) and the low separability values of some classes of the oak crown colors that are shown in Table 1 indicated that the results of the digital classification may have been subject to errors despite the careful selection of the reference trees. All of the separability measures indicated that the separation of the yellow oaks (Y) from the yellow-brown oaks (Y/B) and the green oaks (G) from the green-yellow oaks (G/Y) may have proven to be the most difficult.

The classifications that were made using the MD, ML, Fisher, and kNN algorithms were so-called pixel classifications; i.e., the classified objects were pixels in three orthomosaic channels based on their brightness and not entire tree crowns (as was the case in the field and visual classifications that were made by the observers). These were, therefore, two fundamentally different approaches to the task of classification. Within the crown of a single tree, there were several dozen or even several hundred pixels; as a result of the pixel classification, they could have been categorized into different classes. This was indeed the case (Fig. 5). To overcome this problem, a procedure was proposed to classify the entire collection of tree crowns into one of the five classes of colors by adopting the class that was the most numerous within a given crown (Fig. 6).

In order to compare the obtained results, histograms were made of the tree distributions in the color classes of their crowns in all of the variants of classification (Fig. 7). Comparing the histograms, it can be seen that the most-similar results were obtained in the ML and Fisher methods, followed by kNN. These three classifications gave results that were similar to those that were obtained during the classification that was performed in the field. The MD classification differed significantly from all of the other results. The manual classification that was performed by the observer with the use of the orthomosaic differed from both the results of the classification that was performed in the field and those from the uses of the ML, Fisher, and kNN digital classifications.

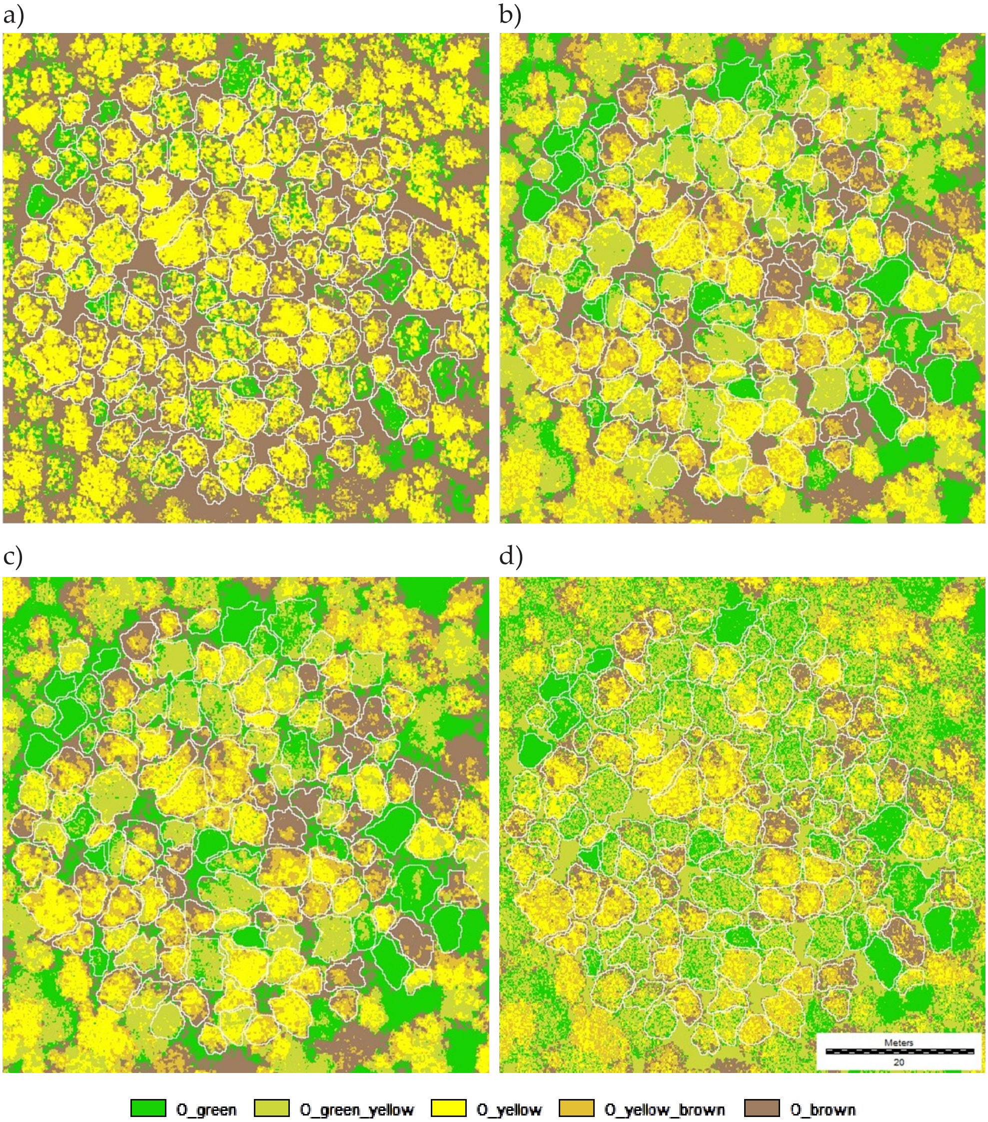


**Fig. 5.** Pixel-classification results using digital classification: a) MD; b) ML; c) Fisher; d) kNN

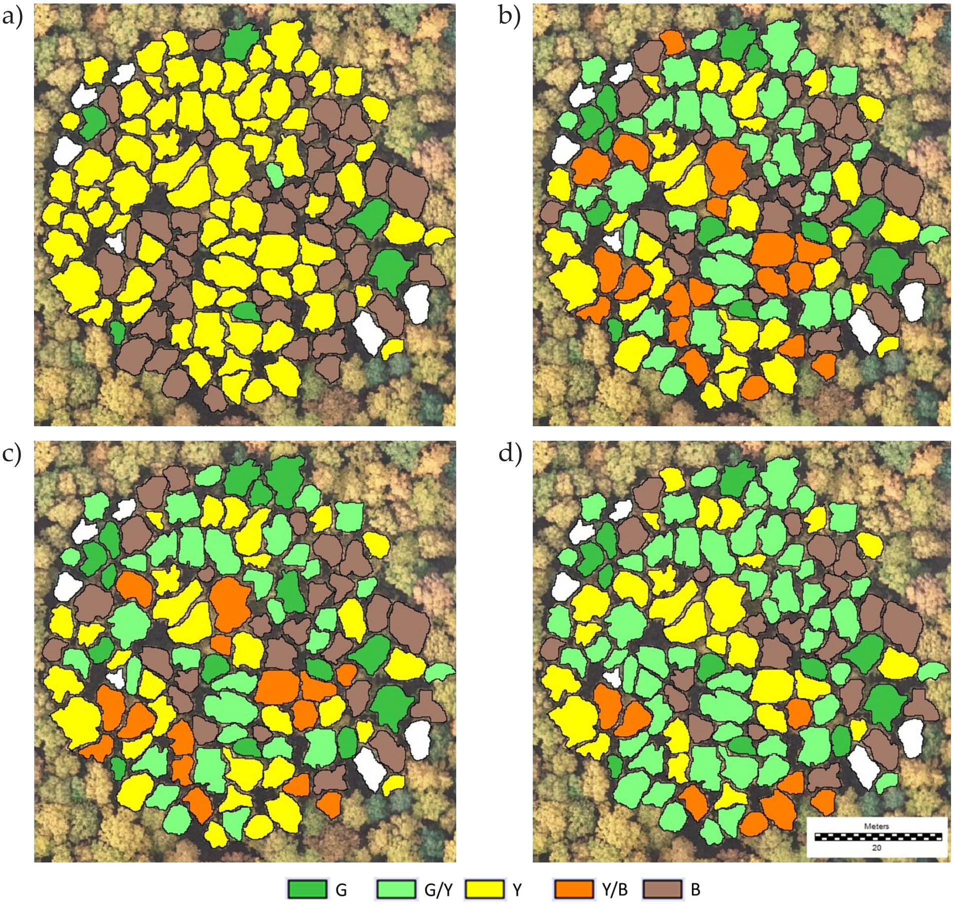


**Fig. 6.** Results of reclassification of trees by adopting entire crown of class that was most represented in digital classification: a) MD; b) ML; c) Fisher; d) kNN

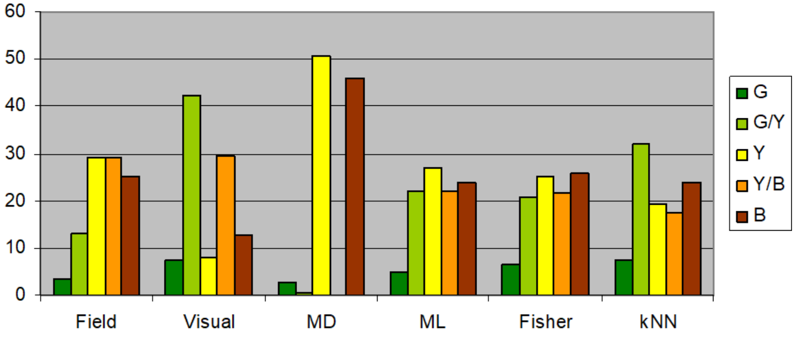


**Fig. 7.** Shares [%] of oaks in individual classes of leaf colors according to applied classification procedures: field observations, visual classification on orthomosaic, and MD, ML, Fisher, and kNN digital classifications

### 3.4. Contingency Analysis

In order to accurately compare the classifications, contingency tables have been introduced to this document; these make it possible to show how those oaks that belonged to the different classes of crown colors were categorized in the classification methods that were used. Table 2 shows the results when field data was used as a reference, while Table 3 compares the classification results with the visual classification that was performed on the orthomosaic. Then, two measures of accuracy that are commonly used in remote sensing were calculated: overall accuracy (OA), and kappa [34].

Overall accuracy determines the share of correctly classified trees; i.e., this is the sum of the numbers that lie on the diagonal of the matrix divided by the number of all of the analyzed trees. The kappa analysis was designed to assess to what extent the results of a classification are better than random assignment. Both measures may take on values within a range of 0 to 1; i.e., from a complete discrepancy between the results of the two classifications to their full agreement.

**Table 2.** Contingency matrix that compares visual and digital-image-classification results with field data

| Classificationon orthomosaic | | Field classification (reference) | | | | | |
|---|---|---|---|---|---|---|---|
| | | G | G/Y | Y | Y/B | B | Sum |
| Visual<br>OA = 35.25%<br>Kappa = 0.189539 | G | 10 | 11 | 5 | 3 | 3 | 32 |
| | G/Y | 3 | 36 | 77 | 47 | 10 | 173 |
| | Y | 0 | 2 | 16 | 9 | 6 | 33 |
| | Y/B | 1 | 6 | 21 | 48 | 49 | 125 |
| | B | 0 | 0 | 1 | 16 | 37 | 54 |
| | Sum | 14 | 55 | 120 | 123 | 105 | 417 |
| Minimum distance<br>OA = 37.89%<br>Kappa = 0.157471 | G | 7 | 5 | 0 | 0 | 0 | 12 |
| | G/Y | 0 | 0 | 0 | 1 | 1 | 2 |
| | Y | 5 | 30 | 80 | 59 | 34 | 208 |
| | Y/B | 0 | 0 | 0 | 0 | 0 | 0 |
| | B | 2 | 20 | 39 | 63 | 71 | 195 |
| | Sum | 14 | 55 | 119 | 123 | 106 | 417 |
| Maximum likelihood<br>OA = 45.80%<br>Kappa = 0.292616 | G | 7 | 8 | 2 | 2 | 2 | 21 |
| | G/Y | 6 | 29 | 34 | 20 | 2 | 91 |
| | Y | 0 | 10 | 56 | 32 | 13 | 111 |
| | Y/B | 1 | 6 | 21 | 38 | 27 | 93 |
| | B | 0 | 2 | 7 | 31 | 61 | 101 |
| | Sum | 14 | 55 | 120 | 123 | 105 | 417 |

**Table 2.** cont.

| Classificationon orthomosaic | | Field classification (reference) | | | | | |
|---|---|---|---|---|---|---|---|
| | | G | G/Y | Y | Y/B | B | Sum |
| Fisher<br>OA = 46.76%<br>Kappa = 0.307941 | G | 9 | 12 | 2 | 3 | 2 | 28 |
| | G/Y | 4 | 26 | 34 | 19 | 3 | 86 |
| | Y | 0 | 9 | 54 | 28 | 11 | 102 |
| | Y/B | 1 | 6 | 22 | 40 | 23 | 92 |
| | B | 0 | 2 | 8 | 33 | 66 | 109 |
| | Sum | 14 | 55 | 120 | 123 | 105 | 417 |
| kNN<br>OA = 40.53%<br>Kappa = 0.244482 | G | 9 | 13 | 2 | 5 | 2 | 31 |
| | G/Y | 4 | 30 | 56 | 31 | 9 | 130 |
| | Y | 0 | 8 | 36 | 25 | 13 | 82 |
| | Y/B | 1 | 3 | 18 | 32 | 19 | 73 |
| | B | 0 | 1 | 8 | 30 | 62 | 101 |
| | Sum | 14 | 55 | 120 | 123 | 105 | 417 |

**Table 3.** Contingency matrix that compares digital-image-classification results with visual classification on orthomosaic

| Digital classification on orthomosaic | | Visual classification on orthomosaic (reference) | | | | | |
|---|---|---|---|---|---|---|---|
| | | G | G/Y | Y | Y/B | B | Sum |
| Minimum distance<br>OA = 23.98%<br>Kappa = 0.145906 | G | 12 | 0 | 0 | 0 | 0 | 12 |
| | G/Y | 0 | 2 | 0 | 0 | 0 | 2 |
| | Y | 6 | 116 | 33 | 52 | 1 | 208 |
| | Y/B | 14 | 0 | 0 | 0 | 0 | 14 |
| | B | 0 | 55 | 0 | 73 | 53 | 181 |
| | Sum | 32 | 173 | 33 | 125 | 54 | 417 |
| Maximum likelihood<br>OA = 57.55%<br>Kappa = 0.460192 | G | 18 | 3 | 0 | 0 | 0 | 21 |
| | G/Y | 14 | 75 | 1 | 0 | 1 | 91 |
| | Y | 0 | 76 | 25 | 10 | 0 | 111 |
| | Y/B | 0 | 17 | 7 | 69 | 0 | 93 |
| | B | 0 | 2 | 0 | 46 | 53 | 101 |
| | Sum | 32 | 173 | 33 | 125 | 54 | 417 |

**Table 3.** cont.

| | | | | | | | |
|---|---|---|---|---|---|---|---|
| Fisher<br>OA = 58.75%<br>Kappa = 0.477851 | G | 23 | 5 | 0 | 0 | 0 | 28 |
| | G/Y | 9 | 76 | 0 | 0 | 1 | 86 |
| | Y | 0 | 66 | 28 | 8 | 0 | 102 |
| | Y/B | 0 | 22 | 5 | 65 | 0 | 92 |
| | B | 0 | 4 | 0 | 52 | 53 | 109 |
| | Sum | 32 | 173 | 33 | 125 | 54 | 417 |
| kNN<br>OA = 62.11%<br>Kappa = 0.505071 | G | 23 | 6 | 0 | 1 | 1 | 31 |
| | G/Y | 9 | 111 | 1 | 9 | 0 | 130 |
| | Y | 0 | 37 | 24 | 21 | 0 | 82 |
| | Y/B | 0 | 17 | 8 | 48 | 0 | 73 |
| | B | 0 | 2 | 0 | 46 | 53 | 101 |
| | Sum | 32 | 173 | 33 | 125 | 54 | 417 |

## 4. Discussion of Results and Conclusions

All of the results of the digital classification that was performed on the orthomosaic showed a relatively low agreement with the field and visual classifications. On the basis of Figure 7, it can be assumed that the digital classification was more consistent with the field classification; however, this was not confirmed by the contingency matrices (Tables 2, 3). The values of both the overall accuracy and the kappa index were very low and quite distant from the satisfactory level of approx. 85–90% that is assumed in remote sensing. The occurrences of the differences in the results of the performed tree classifications was inevitable: first, the field and orthomosaic observations were made by two distinct observers; both of these variants carry a significant load of subjectivism when assessing such a subtle phenomenon as color. It should be remembered that the observers saw the trees from different perspectives – from the profile in the field, and orthogonally from above on the orthomosaic. The observer who worked on the photos had a better opportunity to compare the observed trees with the other specimens and had a lot of time to perform his activities; however, the observer who worked in the field had a brief contact with each tree, thus limiting the possibilities of comparisons with the other trees. Moreover, he saw the trees (especially, their top parts) against the background of a bright sky, which interfered with the correct performance of the classification. In both cases, the observers sometimes saw zones of different colors within the crowns, and it was necessary to classify each tree into only one class of foliage color. This may have been the reason why the digital classifications (except for MD) were better-matched by the visual classification on the orthomosaic (Table 3) than by the field classification (Table 2). The visual classification on the orthomosaic showed little consistency with the field classification. In the manual classification on the orthomosaic, a relatively high number of trees that were categorized as G/Y and Y/B were obtained as compared to those in the G, Y, and B classes (Fig. 7). In the other classification methods (except for MD), more-even distributions were obtained. This result may have been interpreted in such a way that the observer who performed the manual classification on the orthomosaic likely had his own relatively 'sharp' mental criterion for distinguishing the yellow color (Y); as a result, those trees with crown colors that even slightly deviated from this 'pattern' were classified to the transitional (intermediate) G/Y and Y/B colors.

Digital classification may be considered to be objective (although, with some caveats). As supervised classification procedures, they require the indications of reference and training objects and, thus, the involvement of an observer. Both the selections of model trees and their numbers and crown sizes are important, as these affects the sample sizes (the numbers of trees, and the numbers of pixels). The results that are obtained by pixel classification are not unambiguous for individual trees; this is due to the variability of the colors within a canopy as well as the lighting conditions. In particular, the lighting conditions are responsible for the significant stretching of the ellipses that describe the dispersion of the brightness values of the pixels of any reference trees (Fig. 4). In our tests, this fact contributed to obtaining a completely different result of the MD classification when compared to the other methods.

When switching from pixel classification to whole-canopy classification, a criterion was used that was based on the abundance of the most common pixel class in a given tree canopy; in other words, it was a modal or majority value that was calculated for the pixels that were located within the contours of the individual trees. As has been shown, the results of the ML, Fisher, and kNN methods were similar when comparing these methods with each other, and they showed similarities to the classification that was performed in the field.

The problem of relating the obtained results to the data that could have been considered to be the reference level should be discussed separately. Placing the results of the classification that was performed in the field in this role may need to be questioned due to the previously demonstrated difficulties in observing the tree crowns. On the other hand, the classification that was made by the observer on the orthomosaic may have been burdened with considerable subjectivism when distinguishing the colors (which was also mentioned above). The experiences of observing many other similar materials showed that the color diversity of the trees was very well visible from the low-altitude remote-sensing ceiling. From this level, the classified trees may have been compared with almost all of the others, which may have helped to decide what was particularly important when choosing our reference trees.

The process of the changing of the colors of tree crowns is a continuous process, not a step change. This continuity is clearly visible in the color space (Fig. 4), because the ellipses of the pixel distributions of the master trees occupy positions that form certain sequences. This is similar to the sequence of changes in colors and, more broadly, the brightness of pixels in different spectral channels that can be observed as cereals ripen, for example. Therefore, knowing the brightness values for the G, Y, and B colors of tree crowns, it is possible to predict the values that are typical for crowns with transitional colors; i.e., G/Y and Y/B. When attempting to analyze the phenomenon of autumnal changes in the colors of tree crowns, it is therefore recommended to utilize digital classification – provided that the reference objects are carefully selected. It is also worth considering whether it is necessary to be very detailed in the classification (i.e., whether it is not worth limiting this to the main colors; e.g., G, Y, B); however, it is known that, in the cases of other tree species, there may be a clear phase of red coloration. Therefore, the decision on selecting the color sequence should be preceded each time by careful field observations of their changes over time.

In this study, spectral indices that are normally used in the study of phenological phenomena were not utilized. Channels from visible and other ranges (such as infrared) could have been used to calculate them, but this aspect was not considered; in view of the development of low-altitude hyperspectral remote-sensing technology, however, this is worth taking into account in future research. Low-altitude RGB images that are taken with UAVs may be used to analyze the course of an analogous phenomenon in other tree species – especially, maples and beech.

**Funding**

The study was based on images and field data that was acquired during project 505-10-03260052, "Assessment of the pine stands health on the basis of non-metric multispectral digital images obtained with an unmanned aerial vehicle," which was funded by the Warsaw University of Life Sciences – SGGW in 2011 (Head: Krzysztof Stereńczak). The visual classification of oaks on an orthomosaic as well as the digital classification and final elaboration of the topic of this article were carried out as part of author's own research that was conducted at the University of Lodz, Poland.

**Declaration of Competing Interests**

The author declares that he has no known competing financial interests or personal relationships that could have appeared to influence the work that is reported in this paper.

**Data Availability**

There is no public access to the data used in this research. Data may be made available by the author for research purposes upon reasonable request.

**Use of Generative AI and AI-Assisted Technologies**

No generative AI or AI-assisted technologies were employed in the preparation of this manuscript.

## References

[1] Stachak A.: *Dwie fenologiczne formy buka w Puszczy Bukowej pod Szczecinem oraz w Szczecinie* [Two phenological forms of beech in the Beech Forest near Szczecin and in Szczecin itself]. Sylwan, vol. 112(8), 1968, pp. 59–62.

[2] Fijałkowski D.: *Zmienność dębów szypułkowego (Quercus robur L.) i bezszypułkowego (Quercus sessilis Ehrh.) w lasach Lubelszczyzny* [Variation of pedunculate (Quercus robur L.) and durmast (Quercus sessilis Ehrh.) oaks in forests of Lublin province]. Sylwan, vol. 112(12), 1968, pp. 41–47.

[3] Fijałkowski D.: *Badania nad okresami rozwijania się i zrzucania liści u dębu szypułkowego Quercus robur L.* [Studies of periods of developing and falling down of leaves in Quercus robur L.]. Annales Universitatis Mariae Curie-Skłodowska. Sectio C, Biologia, vol. 23, 1968, pp. 203–212.

[4] Hernik I.: *Fenologiczne formy dębu szypułkowego* [Phenological forms of the English oak]. Sylwan, vol. 117(7), 1973, pp. 61–69.

[5] Dolnicki A., Kraj W.: *Leaf morphology and the dynamics of frost-hardiness of shoots in two phenological forms of European beech (Fagus silvativa L.) from southern Poland*. Electronic Journal of Polish Agricultural Universities, Forestry, vol. 4(2), 2001, 01. http://www.ejpau.media.pl/volume4/issue2/forestry/art-01.html.

[6] Chmura D.J.: *Fenologia wiosennego rozwoju polskich proweniencji dębu szypułkowego (Quercus robur L.) i bezszypułkowego (Q. petraea [Matt.] Liebl.)* [Bud burst phenology of Polish provenances of pedunculate (Quercus robur L.) and sessile (Q. petraea [Matt.] Liebl.) oaks]. Sylwan, vol. 146(4), 2002, pp. 97–103.

[7] Crawley M.J., Akhteruzzaman M.: *Individual variation in the phenology of oak trees and its consequences for herbivorous insects.* Functional Ecology, vol. 2(3), 1988, pp. 409–415. https://doi.org/10.2307/2389414.

[8] Csóka G.: *Variation in Quercus robur susceptibility to galling wasps (Hymenoptera: Cynipidae) linked to tree phonology*, [in:] Prince P.W., Mattson W.J., Baranchikov Y.N. (eds.), *The Ecology and Evolution of Gall-Forming Insects [Microform]*, General Technical Report NC-174, U.S. Department of Agriculture, Forest Service, North Central Forest Experiment Station, St. Paul, pp. 148–152.

[9] Mopper S., Simberloff D.: *Differential herbivory in an oak population: The role of plant phenology and insects performance*. Ecology, vol. 76(4), 1995, pp. 1233–1241. https://doi.org/10.2307/1940930.

[10] Visser M.E., Holleman L.J.M.: *Warmer springs disrupt the synchrony of oak and winter moth phenology*. Proceedings of the Royal Society B: Biological Sciences, vol. 268(1464), 2001, pp. 289–294. https://doi.org/10.1098/rspb.2000.1363.

[11] Waddell K.J., Fox C.W., White K.D., Mousseau T.A.: *Leaf abscission phenology of a scrub oak: consequences for growth and survivorship of a leaf mining beetle.* Oecologia, vol. 127(2), 2001, pp. 251–258. https://doi.org/10.1007/s004420000576.

[12] Kot I., Rubinowska K., Michałek W.: *Changes in chlorophyll fluorescence and pigments composition in oak leaves with galls of two cynipid species (Hymeniptera, Cnipidae)*. Acta Scientiarum Polonorum Hortorum Cultus, vol. 17(6), 2018, pp. 147–157. https://doi.org/10.24326/asphc.2018.6.15.

[13] Ekholm A., Tack A.J.M., Bolmgren K., Roslin T.: *The forgotten season: the impact of autumn phenology on a specialist insect herbivore community on oak*. Ecological Entomology, vol. 44(3), 2019, pp. 425–435. https://doi.org/10.1111/een.12719.

[14] Morin X., Roy J., Sonié L., Chuine I.: *Changes in leaf phenology of three European oak species in response to experimental climate change*. New Phytologist, vol. 186(4), 2010, pp. 900–910. https://doi.org/10.1111/j.1469-8137.2010.03252.x.

[15] Vitasse Y., Delzon S., Dufrêne E., Pontailler J.-Y., Louvet J.-M., Kremer A., Michalet R.: *Leaf phenology sensitivity to temperature in European trees: Do within-species populations exhibit similar responses?* Agricultural and Forest Meteorology, vol. 149(5), 2009, pp. 735–744. https://doi.org/10.1016/j.agrformet.2008.10.019.

[16] Vitasse Y., François C., Dolpierre N., Dufrêne E., Kremer A., Chuine I., Delzon S.: *Assessing the effects of climate change on the phenology of European temperate trees*. Agricultural and Forest Meteorology, vol. 151(7), 2011, pp. 969–980. https://doi.org/10.1016/j.agrformet.2011.03.003.

[17] Fisher J.I., Mustard J.F., Vadeboncoeur M.A.: *Green leaf phenology at Landsat resolution: Scaling from the field to the satellite*. Remote Sensing of Environment, vol. 100(2), 2006, pp. 265–279. https://doi.org/10.1016/j.rse.2005.10.022.

[18] Polgar C.A., Primack R.B.: *Leaf-out phenology of temperate woody plants: From trees to ecosystems*. New Phytologist, vol. 191(4), 2011, pp. 926–941. https://doi.org/10.1111/j.1469-8137.2011.03803.x.

[19] Lisein J., Michez A., Claessens H., Lejeune P.: *Discrimination of deciduous tree species from time series of unmanned aerial system imagery*. PLoS ONE, vol. 10(11), 2015, e0141006. https://doi.org/10.1371/journal.pone.0141006.

[20] Będkowski K., Stereńczak K.: *Sessile oak (Quercus petraea (Mattuschka) Liebl.) trees variability according to an analysis of multispectral images taken from UAV – first results*. Ecological Questions, vol. 17, 2013, pp. 25–33. https://doi.org/10.12775/ecoq-2013-0013.

[21] Łoziński A., Będkowski K.: *Rozpoznawanie jesiennych faz fenologicznych dębu bezszypułkowego (Quercus petraea Liebl.) na ortomozaikach zdjęć lotniczych uzyskanych z wykorzystaniem drona* [Monitoring of sessile oak (Quercus petraea Liebl.) autumn phenology using orthomosaics made on a basis of aerial images acquired with drone]. Teledetekcja Środowiska, t. 55, 2016, pp. 5–14.

[22] Będkowski K., Szymański P.: *Dynamics of autumn discoloration of tree crowns in sessile oak stand based on the time series of low-altitude aerial photographs*. Sylwan, vol. 167(10), 2023, pp. 650–665. https://doi.org/10.26202/sylwan.2023027.

[23] Boyer M., Miller J., Belanger M., Hare E, Wu J.: *Senescence and spectral reflectance in leaves of northern pin oak (Quercus palustris Muenchh)*. Remote Sensing of Environment, vol. 25(1), 1988, pp. 71–87. https://doi.org/10.1016/0034-4257(88)90042-9.

[24] Olędzki J.R.: *Badania zróżnicowania własności optyczno-spektralnych środowiska geograficznego* [Studies on differentiation of optical spectral properties of geographic environment]. Teledetekcja Środowiska, t. 23, 1993, pp. 7–35.

[25] Demarez V., Gastellu-Etchegorry J.P., Mougin E., Marty G., Proisy C., Dufrêne E., Le Dantec V.: *Seasonal variation of leaf chlorophyll content of a temperate forest. Inversion of the PROSPECT model.* International Journal of Remote Sensing, vol. 20(5), 1999, pp. 879–894. https://doi.org/10.1080/014311699212975.

[26] Merzlyak M.N., Gitelson A.A., Chivkunova O.B., Rakitin V.Yu.: *Non-destructive optical detection of pigment changes during leaf senescence and fruit ripening*. Physiologia Plantarum, vol. 106(1), 1999, pp. 135–141. https://doi.org/10.1034/j.1399-3054.1999.106119.x.

[27] Sims D.A., Gamon J.A.: *Relationships between leaf pigment content and spectral reflectance across a wide range of species, leaf structures and developmental stages.* Remote Sensing of Environment, vol. 81(2–3), 2002, pp. 337–354. https://doi.org/10.1016/S0034-4257(02)00010-X.

[28] Estrella N., Menzel A.: *Responses of leaf colouring in four deciduous tree species to climate and weather in Germany*. Climate Research, vol. 32, 2006, pp. 253–267. https://doi.org/10.3354/cr032253.

[29] Keskitalo J., Bergquist G., Gardeström P., Jansson S., 2005. *A cellular timetable of autumn senescence*. Plant Physiology, vol. 139(4), 2005, pp. 1635–1648. https://doi.org/10.1104/pp.105.066845.

[30] Lim P.O., Kim H.J., Nam H.G.: *Leaf senescence*. Annual Review of Plant Biology, vol. 58, 2007, pp. 115–136. https://doi.org/10.1146/annurev.arplant.57.032905.105316.

[31] University of Haifa: *Why more autumn leaves are red in America and yellow in Europe: New theory*. ScienceDaily, 17 August 2009. https://www.sciencedaily.com/releases/2009/08/090813142150.htm [access: 10.08.2024].

[32] Plutecki W., Zmarz A., Sanko I.: *A truly photogrammetric UAV*. GIM International, no. 4, 2013. https://www.gim-international.com/content/article/a-truly-photogrammetric-uav [access: 28.06.2024].

[33] Clark University. Center for Geospatial Analytics: *TerrSet*. https://www.clarku.edu/centers/geospatial-analytics/terrset/ [access: 25.02.2025].

[34] Congalton R.S.: *A review of assessing the accuracy of classifications of remotely sensed data*. Remote Sensing of Environment, vol. 37(1), 1991, pp. 35–46. https://doi.org/10.1016/0034-4257(91)90048-B.